Magnetic nanoelements for magnetoelectronics made by focused-ion-beam milling

Gang Xiong,[a] D. A. Allwood, M. D. Cooke, and R. P. Cowburn
Nanomagnetism Group, Department of Physics, University of Durham, Rochester Building, Science Laboratories, South Road, Durham DH1 3LE, United Kingdom

(Received 23 July 2001; accepted for publication 26 September 2001)

Focused-ion-beam (FIB) milling has been used to structure magnetic nanoelements from 5 nm thick films of permalloy. We have used focused 30-keV Ga^+ ions to define small arrays ($6\,\mu m \times 6\,\mu m$) of wires, circles, and elongated hexagons in the size range 100–500 nm. High-sensitivity magneto-optical measurements combined with atomic force microscopy show that very high quality magnetic nanostructures can be fabricated by FIB milling even in thin films of soft magnetic materials. This finding could be significant for the future commercialization of certain aspects of magnetic nanotechnology and magnetoelectronics. © *2001 American Institute of Physics.* [DOI: 10.1063/1.1419032]

Focused-ion-beam (FIB) irradiation and milling are very versatile and rapid laboratory techniques for laterally structuring materials into devices.[1,2] In some cases, fabrication rates may even be high enough to additionally consider using FIB for the commercial production of nanostructures. Recently, FIB milling has been demonstrated to be capable of producing high quality magnetic nanostructures from magnetically *hard* thin films.[3] However, for magnetically *soft* materials, such as those used in the emerging technology of magnetoelectronic devices, the degree to which the magnetic properties of the structured devices suffer due to FIB milling remains unclear. Ion implantation, the introduction of magnetic pinning defects, and nanometer-scale displacements are all ion-induced mechanisms which have recently been shown to strongly influence soft magnetic properties.[2] We have attempted to address this uncertainty and here report an experimental investigation on the use of FIB milling to fabricate magnetic nanostructures from permalloy ($Ni_{80}Fe_{20}$).

We have used FIB milling to structure a thin permalloy film into a variety of technologically important structures, including long planar wires (for position sensing),[4] elongated hexagons (for magnetic memory cells),[5] and circular dots (for magnetic field sensing and logic devices).[6] Atomic force microscopy (AFM) has been used for structural characterization of the nanostructures and magneto-optical Kerr effect (MOKE) magnetometry has provided a probe of their magnetic properties. We show experimentally that the magnetic properties of these nanostructures are very good indeed and, consequently, that FIB milling is an excellent nanofabrication technique even in thin films of soft magnetic materials.

The permalloy films were grown by vacuum thermal evaporation at a rate of $0.1\,nm\,s^{-1}$ to a thickness of 5 nm on a (100) oriented single-crystal silicon substrate. The base pressure in the vacuum chamber was 1×10^{-8} mbar which rose to 1×10^{-6} mbar during evaporation. The permalloy layer was then patterned by a FEI 200 xP® FIB workstation using a Ga^+ liquid metal ion source operated at 30-keV ion energy.

In order to calibrate the FIB milling rate, $100\,\mu m \times 100\,\mu m$ square areas of the permalloy film were irradiated with different ion doses. This was performed using an ion beam current of 3 nA (probe diameter = 27 nm) and milling times between 0 and 43 s per square area to provide dose densities ranging from 0 to $13\,C\,m^{-2}$. AFM was performed using a Digital Instruments 3a Nanoscope SPM instrument, with a silicon nitride tip, in contact mode. A high-sensitivity longitudinal MOKE magnetometer,[7] with a focused laser spot diameter of $\sim5\,\mu m$, was then used to obtain room temperature $M-H$ hysteresis loops from the milled areas.

Figure 1(a) shows the milling depth, measured by the AFM as a function of FIB dose density, D, and reveals two milling regimes with different etch rates. We attribute the first region ($D<6\,C\,m^{-2}$; etch rate $=0.8\,nm\,C^{-1}\,m^2$) to the removal of permalloy and the second ($D>6\,C\,m^{-2}$; etch rate $=0.38\,nm\,C^{-}\,m^2$) to milling of the underlying Si substrate. This is supported by the etch rate changing at a mill depth of 5 nm, equal to the permalloy film thickness. Figure 1(b) shows the measured coercivity, H_C, and the Kerr signal expressed as a percentage change in intensity, from the uniformly milled $100\,\mu m \times 100\,\mu m$ windows. The Kerr signal decreases approximately linearly with increasing D and reaches zero at $D=5.6\,C\,m^{-2}$ [Fig. 1(b)], which is consistent with the thickness of the magnetic layer being progressively reduced by milling. The initial decrease of H_C with D is explained by the reduction in magnetic domain wall energy as the film thickness is reduced, and hence, lower domain nucleation and propagation fields. Ion-induced annealing of magnetic defects will also play a role in this reduction. However, beyond $D=1.4\,C\,m^{-2}$, H_C increases again, possibly due to the film roughness becoming more significant as the film thickness decreases, leading to increased domain wall pinning. The subsequent rapid decrease of H_C for $3.7\,C\,m^{-2}<D<4.9\,C\,m^{-2}$ can be attributed to the onset of superparamagnetism as the film becomes noncontinuous.

Once dose calibration was complete, small $6\,\mu m \times 6\,\mu m$ arrays comprising identical nanostructures were patterned into fresh areas of the same permalloy film using an

[a]Electronic mail: gang.xiong@durham.ac.uk

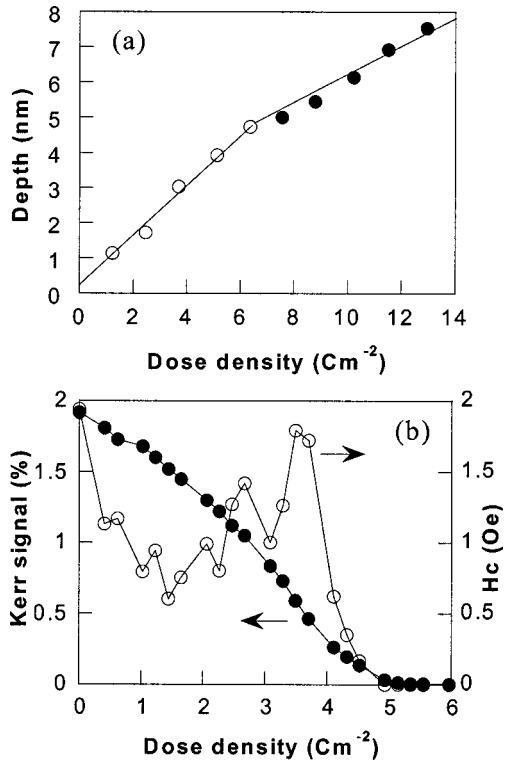

FIG. 1. The dependence of (a) milled depth as measured by AFM, and (b) coercivity, H_C, and Kerr signal amplitude, upon dose density of ion milling of a 5 nm permalloy film on a Si substrate. Two distinct milling rates are visible in (a), corresponding to milling firstly of the permalloy layer (open circles) and secondly the substrate (solid circles).

ion beam current of 10 pA (probe diameter = 10 nm). The first array consisted of 20 planar wires, each wire 6 μm in length and 100 nm wide, maintaining a gap of 300 nm between neighboring wire centres [Figs. 2(a) and 2(b)]. A second array contained a 3×3 array of 1 μm$\times$500 nm elongated hexagons, having a 2 μm distance between element centers [Fig. 2(c)]. The third pattern studied was a 20×20 matrix of circles, each circle having a diameter of 100 nm and a distance of 300 nm between circle centers [Fig. 2(d)]. For each case, the spacing between nanostructures was large enough that magnetostatic interactions between nanostructures could be neglected. Based on Fig. 1(b), we chose a milling dose density of $D = 11\,\mathrm{C\,m^{-2}}$ to ensure that no magnetic material remains after milling. In order to avoid cross talk in the MOKE signal from magnetic switching in the unpatterned magnetic film surrounding the nanostructures, the FIB was programmed to remove all magnetic material around the nanostructures up to a radius of 50 μm from the center of each array.

Figure 3 shows the hysteresis loops measured from the different arrays of nanostructures. In very narrow ferromagnetic wires, the magnetization is restricted to being parallel to the wire axis due to magnetic shape anisotropy. There is evidence that magnetization reversal in such systems usually takes place by nucleation and propagation of a magnetic domain wall at a well-defined reversal field.[8] The very sharp coercive transitions visible in the wire array easy-axis hysteresis loop [Fig. 3(a)—we estimate $<4\%$ standard deviation in the reversal field] are consistent with this model. Most importantly, because the hysteresis loops are averaged across 20 different wires, the sharp coercive transitions also demonstrate a low dispersion in the switching field of different wires. This proves that the FIB-milled wires are of very high quality and that the fabrication process does not introduce defects which strongly influence the magnetic reversal. The hysteresis loop from the easy axis of the elongated hexagon array again shows a very sharp coercive transition [Fig.

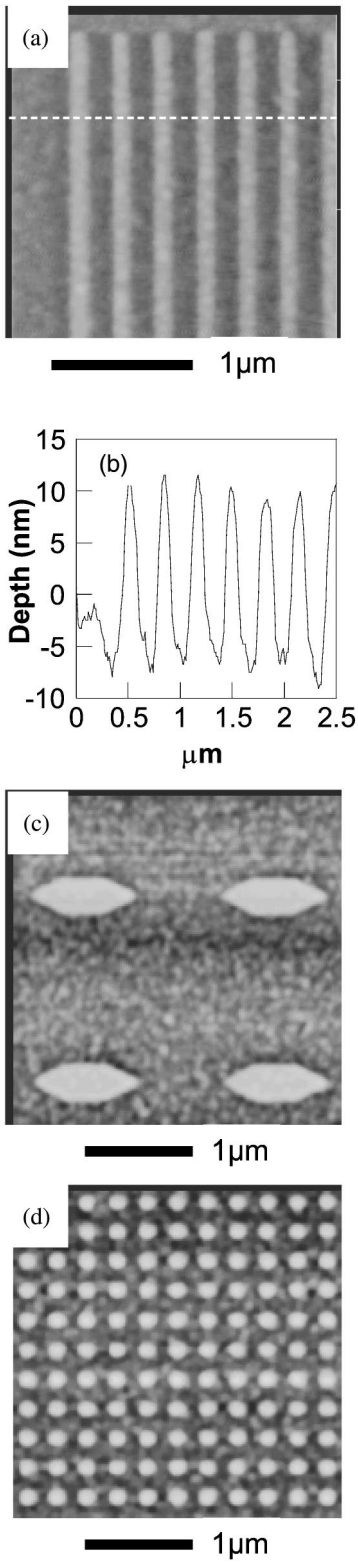

FIG. 2. AFM of different FIB-milled nanostructures: (a) array of wires, 100 nm wide and 6 μm long, (b) AFM cross section measured along the dashed line in panel (a), (c) array of elongated hexagons, 1 μm long and 500 nm wide, and (d) array of circular dots, 100 nm in diameter.

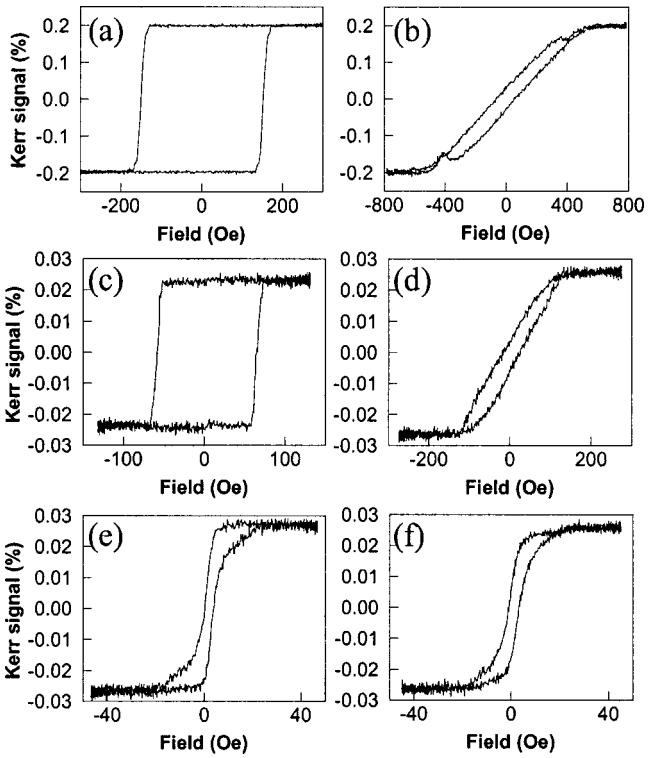

FIG. 3. Magnetic hysteresis loops obtained from different FIB-milled nanostructures: (a) wire array, easy axis; (b) wire array, hard axis; (c) elongated hexagon array, easy axis, (d) elongated hexagon array, hard axis, (e) circular dot array, *x* axis and (f) circular dot array, *y* axis.

3(c)—we estimate $<6\%$ standard deviation in the reversal field]. This is a particularly desirable property for magnetic memory cells. Furthermore, the hard-axis loops of both the wire array and the elongated hexagon array [Figs. 3(b) and 3(d)] show close to model uniaxial hard-axis behavior with low remanence and well-defined saturation fields. This shows that the magnetic reversal of the structures is dominated by their shape anisotropy, and not by magnetic defects. Once again, this suggests that the quality of the nanofabrication is very high. The hysteresis loops from the circular dot array [Figs. 3(e) and 3(f)] were measured at two in-plane directions defined by the orthogonal axes of the array. These loops are similar in appearance, indicating that there is no systematic shape anisotropy to the individual circular nanomagnets. Furthermore, the 2 Oe coercive field and the 15–20 Oe saturation field of the circular dot array are comparable to those measured in a previous study in dots fabricated by high-definition electron-beam lithography.[9] This similarity further supports the suitability of direct FIB patterning for the fabrication of nanoelements from thin films.

In conclusion, we have demonstrated that very high quality magnetic nanostructures can be fabricated by FIB milling even in thin films of soft magnetic materials such as permalloy. No evidence is found for ion-induced damage to the magnetic properties of the nanoelements. The length scales of 100 nm achieved using this rapid fabrication method are suitable for single-domain magnetic devices. This finding allows a high-throughput rate of device fabrication for development work and could even be significant for the future commercialization of certain aspects of magnetic nanotechnology and magnetoelectronics.

The authors are grateful to Eastgate Investment Ltd. for partial support of this work.

[1] C. Chappert, H. Bernas, J. Ferre, V. Kottler, J. P. Jamet, Y. Chen, E. Cambril, T. Devolder, F. Rousseaus, V. Mathet, and H. Launois, Science **280**, 1919 (1998); B. D. Terris, L. Folks, D. Weller, J. E. E. Baglin, A. J. Kellock, H. Rothuizen, and P. Vettiger, Appl. Phys. Lett. **75**, 403 (1999); M. Nakayama, J. Yanagisawa, F. Wakaya, and K. Gamo, Jpn. J. Appl. Phys., Part 1 **38**, 7151 (1999).
[2] W. M. Kaminsky, G. A. C. Jones, N. K. Patel, W. E. Booij, M. G. Blamire, S. M. Gardiner, Y. B. Xu, and J. A. C. Bland, Appl. Phys. Lett. **78**, 1589 (2001).
[3] J. Lohau, A. Moser, C. T. Rettner, M. E. Best, and B. D. Terris, Appl. Phys. Lett. **78**, 990 (2001).
[4] G. A. Prinz, J. Magn. Magn. Mater. **200**, 57 (1999).
[5] G. A. Prinz, Science **282**, 1660 (1998).
[6] R. P. Cowburn and M. E. Welland, Science **287**, 1466 (2000).
[7] R. P. Cowburn, D. K. Koltsov, A. O. Adeyeye, and M. E. Welland, Appl. Phys. Lett. **73**, 3947 (1998).
[8] W. Wernsdorfer, B. Doudin, D. Mailly, K. Hasselbach, A. Benoit, J. Meier, J. Ansermet, and B. Barbara, Phys. Rev. Lett. **77**, 1873 (1996); T. Ono, H. Miyajima, K. Shigeto, K. Mibu, N. Hosoito, and T. Shinjo, Science **284**, 468 (1999).
[9] R. P. Cowburn, D. K. Koltsov, A. O. Adeyeye, and M. E. Welland, Phys. Rev. Lett. **83**, 1042 (1999).